

Transmission THz time domain system for biomolecules spectroscopy

M. P. DINCA, A. LECA^a, D. APOSTOL^a, M. MERNEA^b, O. CALBOREAN^b, D. MIHAILESCU^b, T. DASCALU^{a*}

University of Bucharest, Faculty of Physics

^a*National Institute for Laser, Plasma and Radiation Physics, Laboratory of Solid-State Quantum Electronics, Bucharest R-077125, Romania*

^b*University of Bucharest, Faculty of Biology*

A THz Time Domain Spectroscopy experimental set-up was built for studying the biomolecules absorption spectra in the THz range and obtaining information on their collective motions. Details on the set-up calibration and performances are presented, together with the used noise and artefacts reduction data processing techniques. Preliminary results on the absorbance spectrum of the solvated Bovine Serum Albumin (BSA) for different water concentration are given.

(Received December 15, 2009; accepted January 20, 2010)

Keywords: Terahertz, Terahertz time domain spectroscopy, Terahertz pulsed spectroscopy, Rotational transitions

1. Introduction

Terahertz radiation has gained wide range applications in spectroscopy, imaging and sensing due its non-ionizing, non-invasive, coherent quasi-optic and phase-sensitive properties. An increased interest is observed in using terahertz time-domain spectroscopy (THz-TDS) in biology [1, 2], chemistry [3, 4] and medicine [5, 6] research, such as disease diagnostics, recognition of DNA and biomolecules, and quality control of drugs. As many protein and DNA molecules have distinct signatures in the terahertz spectral region, THz-TDS has been used to identify various types of DNA from low frequency vibrational modes toward label free genetic diagnosis. Various terahertz imaging techniques have been developed in the diagnosis of human and animal tumours such in human skin cancer and basal cell carcinoma [7, 8]. Also, THz time domain spectroscopy is a promising technique for studying the collective vibrational modes of biomolecules and getting a better understanding of the relationship between their conformation and biological function [9-11].

Here we report a THz-TDS system built for biomolecules spectral investigation; various sources of noise and systematic errors are analyzed and the data processing trying to minimize their effect are presented. Preliminary results on bovine serum albumin (BSA) are given, as well.

2. Experimental set-up

The diagram of the experimental setup for THz-TDS is presented in Fig. 1. A femtosecond (fs) pulse train is emitted from a self mode locked fiber laser (TOPTICA

GmbH) SHG having the following specifications: 780nm wavelength, 80mW average power, 150 fs pulse length.

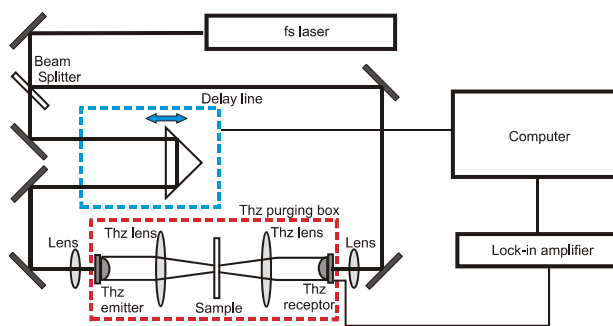


Fig. 1. TDS-THz setup for pulse transmission measurements.

The optical pulse train having a 90 MHz repetition rate encounters a beam-splitter and is separated in two equivalent beams. One beam travels to the THz source, a DC biased microstrip photoconductive antenna fabricated on low-temperature grown GaAs (LT-GaAs) 400 μm thick substrate, and is focused by an integrated silicon lens between the electrodes where THz pulses are produced when optical excitation induces conductivity changes in semiconductor. The maximum bias voltage is 80 V and typical emitted average power of THz radiation is 10 μW when pumped by mode-locked ultra fast laser with 80 mW output power. The THz pulse is then focused using polyethylene lens onto the sample, where the interaction between sample and THz radiation may alter the THz pulse shape. The beam emerging from the sample is

expanded by another polyethylene lens and directed onto the THz detector having a structure similar to those of the emitter but working as an unbiased antenna, the photoconductive gap of the antenna being gated by the ultrashort optical pulses of the second beam provided by the beam splitter. The THz pulse provides the bias voltage pulse accelerating the charge carriers to create a current that is amplified and recorded. A delay line based on hollow retro reflector is placed in the pumping beam path to assure pulses synchronization and allow a temporal scan of THz pulses by reconstructing it from time gate measurements. The line is driven by a computer controlled step-motor having the step length of $1.25\mu\text{m}$.

The signal from the THz detector is pre-amplified and then detected by a SR810 DSP lock-in amplifier (Stanford Research Systems) using a reference frequency of about 50 kHz to modulate the emitter bias voltage. Through a serial interface the data are transmitted to a personal computer to be recorded and analyzed. The distance between emitter and receiver is about 40 cm. To accommodate the BSA sample a special Teflon holder (Fig. 2) has been designed.

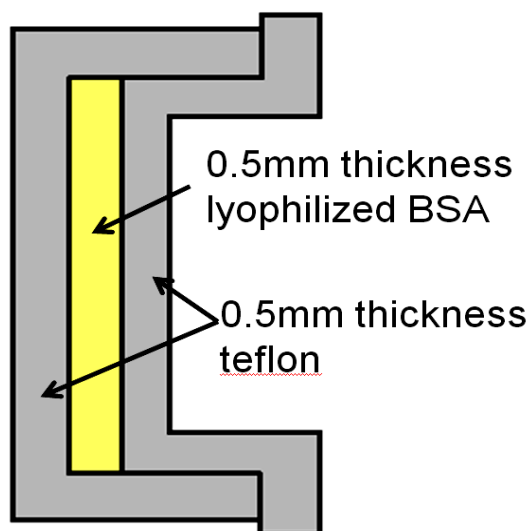
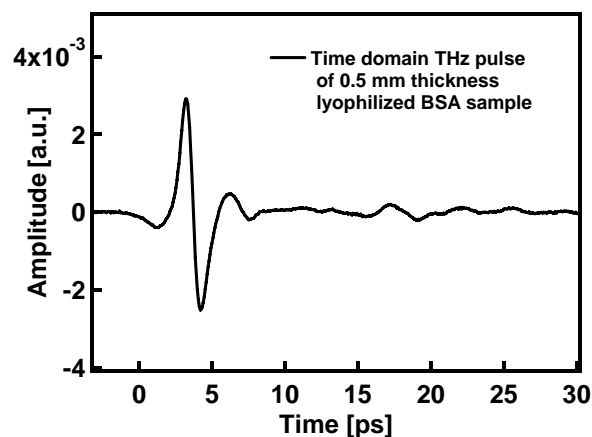


Fig. 2. Teflon holder designed to accommodate the sample.

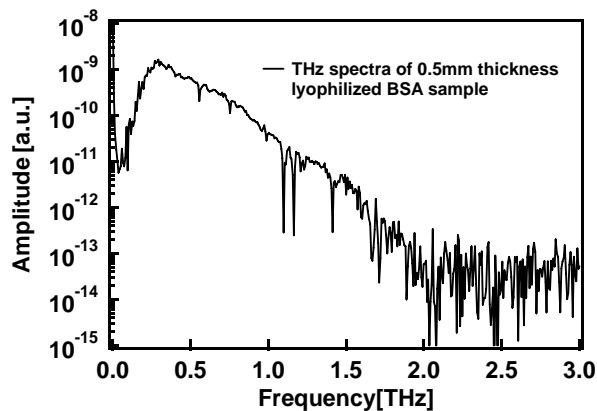
3. Data processing and preliminary results

The detected electrical signal is proportional to the electric field of the terahertz pulse and, by changing the delay between the pumping and gating laser pulses, one can record the terahertz electric field as a function of time. A simple Fourier transformation gives the frequency spectrum. In Fig. 3 typical results of the time waveform and Fourier amplitude obtained for a lyophilized bovine

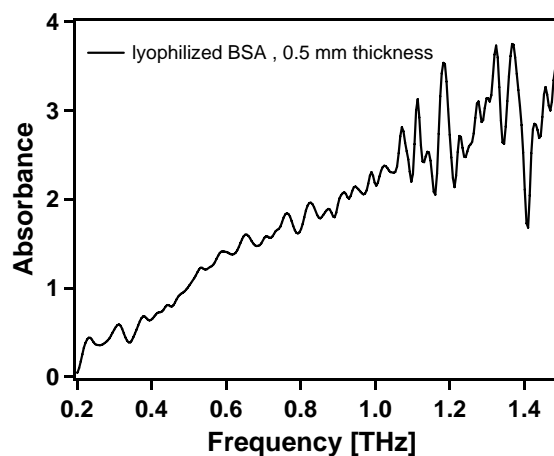
serum albumin (BSA) sample contained in the described Teflon holder are given.



(a)



(b)



(c)

Fig. 3. TDS-THz pulse of 0.5 mm thickness lyophilized BSA sample (a) time-domain, (b) frequency domain, (c) absorbance.

Because the effect of the propagating path is difficult to predict theoretically, two separate measurements are done, without and with the sample included in the THz beam path resulting in $E_{ref}(\omega)$ and $E_{sam}(\omega)$ spectra, respectively. As THz-TDS simultaneously and accurately provide both the Fourier phase and amplitude of waveforms, the complex material properties such as the complex refractive index and dielectric constant can be obtained without complicated Kramers–Kronig analysis. Thus, denoting by $A = \sqrt{R^2 + I^2}$ and $\varphi = \arctan(I/R)$ the magnitude and phase of the ratio of the two complex spectra $R(\omega) + jI(\omega) = E_{sam}(\omega)/E_{ref}(\omega)$, the sample index of refraction can be extracted [12] by

$$n(\omega) = 1 + \frac{c}{\omega d} \varphi(\omega)$$

and

$$k(\omega) = -\frac{c}{\omega d} \ln \left(\frac{(n(\omega) + 1)^2}{4n(\omega)} A \right).$$

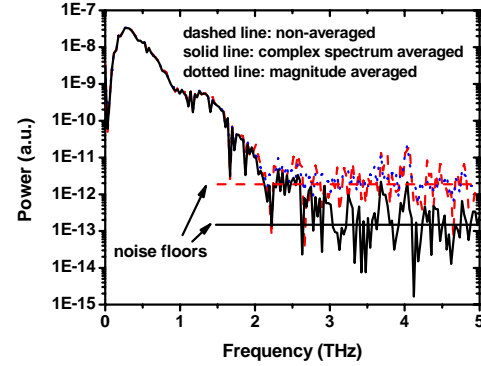
The absorption coefficient α is commonly introduced as

$$\alpha(\omega) = 2 \frac{\omega k(\omega)}{c} = -\frac{2}{d} \ln \left(\frac{(n(\omega) + 1)^2}{4n(\omega)} A \right),$$

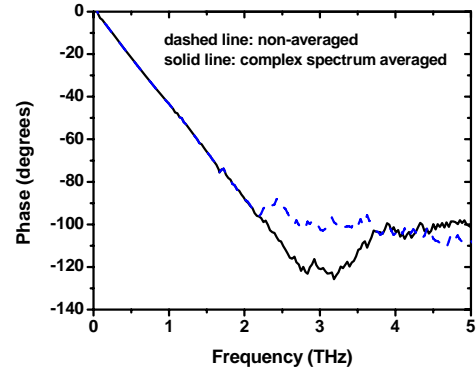
which reduces to $\alpha(\omega) = -\frac{2}{d} \ln A$ if the effect of the entering interface into the sample medium is neglected.

Unfortunately, the THz-TDS measurements can be affected by both random noise and systematic errors. Laser optical noise and short-term stability (on the scale of seconds to minutes) are the primary contributors to random noise in the THz-TDS signal. Fluctuations in the fs laser pulse will exist in the both beam paths of the gated detection scheme, affecting both the generated THz pulse at the source and the current measured at the detector. This increases the standard deviation of the measurement, causing the detection limit to deteriorate.

By averaging multiple records the effect of the high frequency noise can be drastically reduced. Because the observed time jitter is negligible there is no need for a post-record synchronization prior to average the time waveform. The effect of time waveform averaging (or, equivalently, the complex spectra averaging), as apparent in Fig. 4a, is to reduce the amplitude spectrum noise floor. Another way to monitor the averaging effectiveness is the broadening of the spectral region within the phase exhibit a clean behaviour (Fig. 4b). Thus, information up to 2.8 THz can be obtained while without averaging the useful range is up to only 2 THz. By comparison with this, averaging the magnitude of the Fourier spectra results only in a decreasing of fluctuations around the same noise floor level as apparent in Fig. 4 a), dotted line.



(a)



(b)

Fig. 4. Effect of averaging 10 measurement scans on the power and phase spectrum.

For spectroscopic experiments, it is important that the signal remain stable during the acquisition of both the reference and the sample spectrum. If the laser pulse changes dramatically after the reference have been recorded, the sample spectrum will have been acquired under different conditions, and the reference is no longer truly a reference. Taking into account the finite time needed for a spectrum acquisition, this limits the number of the spectra that can be used for averaging.

A primary contributor to systematic error is the presence of atmospheric water vapour. Water vapour has numerous rotational resonances in the THz band. Therefore THz TDS of a sample, in open air, unavoidably results in a combination of the sample spectral features and water vapour resonances in the frequency domain. Thus, spectroscopic results of interest can be obscured. When sample absorbance is measured by taking the ratio of the complex spectra of the sample and the reference, the extremely low amplitude within the water resonances bands makes the noise and other effects dominant and, consequently, can result in large absorbance errors within these bands.

Though the water-vapour effects can be decreased by numerical processing [13] using a resonances model based on a spectroscopic catalog and fine tuning of each resonance, the most effective way for water-vapour removal is to include the THz path in a sealed chamber from where the air is evacuated by nitrogen purging. In Fig. 5a) the spectra obtained for the Teflon holder both in air and nitrogen atmosphere are given clearly indicating the decreasing of the water-vapour effect by nitrogen purging. The absorbance obtained from these spectra (Fig. 5b), show the removal of the water-vapour resonances, as well.

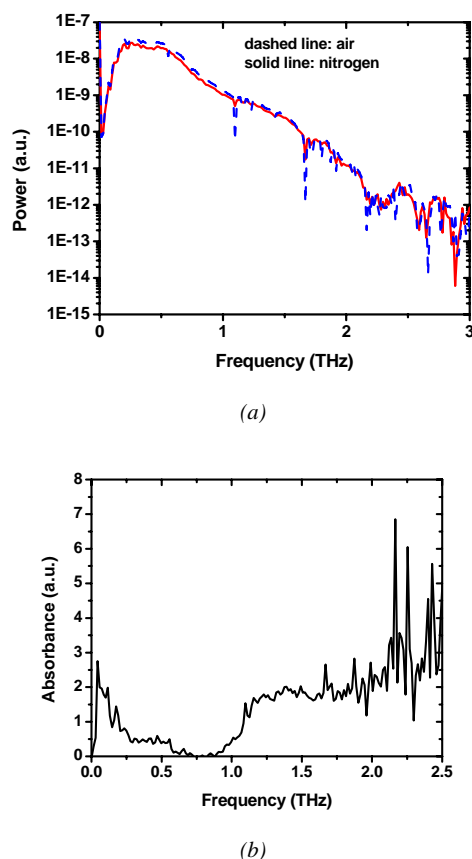


Fig. 5. (a). transmission spectra of the Teflon holder in air (dashed line) and nitrogen (solid line) and (b). holder absorbance as resulted from measurements in nitrogen atmosphere.

Additional errors come from the large spectral range of the THz pulse causing radially variation in the focal plane of spectral components. Besides the above mentioned effects there are additional lines in the transmission spectra generated by sample holder etalon effect. Careful choice of thickness and material is required in order to produce accurate THz spectra.

The delay line can be controlled in steps which have to be multiples of $1.25 \mu\text{m}$ (corresponding to a delay time of $\Delta t = 8.32 \text{ fs}$), the largest available step corresponding

to 66.6 fs . Since the highest frequency in the Digital Fourier Transform (DFT) spectrum is related to the scanning time step by $\nu_{\text{max}} = 1/(2\Delta t)$ [14] and the noise (as can be observed in Fig. 4) obscures the relevant information above 3 THz , a scanning step of 66.6 fs was used during all experiments, providing an analysis band of 7.5 THz and avoiding a too long measurement time. Ten successive scans were averaged, as previously described. The programmed step number (and, consequently, the scan length T_{scan}) determines the spectral resolution in the Fourier spectrum $\Delta\nu = 1/T_{\text{scan}}$. To shorten the measurement time, a number of 1024 scanning steps can be selected, resulting in a spectral resolution of 14.7 GHz (for comparison, the water vapour absorption resonances have linewidths of about 6 GHz).

Using the described setup and data processing method, transmission spectra for solvated BSA (12%, 25%, 34%, 43% and 50%) were obtained with a spectral resolution of 7.4 GHz and investigated in the $0.2\text{-}2.8 \text{ THz}$ range. Two preliminary results of the absorption spectra are presented in Fig. 6.

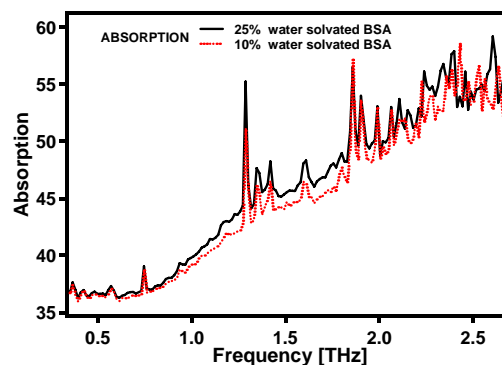


Fig. 6. Absorption spectra of water solvated BSA (10% and 25% water).

4. Conclusions

A THz Time Domain Spectroscopy experimental set-up was built for measuring biomolecules THz absorption spectra. The measured system performances are consistent with those reported in literature for the same kind of emitters/ detectors and involved pumping level. The problem of noise and artefacts caused by the water vapour absorption was addressed both by data processing techniques and experimental set-up improvements. Experiments on different concentration solvated BSA are in progress with the aim to monitor the collective vibrational modes.

References

- [1] T. Löffler, T. Bauer, K Siebert, H. Roskos, A. Fitzgerald, and S. Czasch, *Optics Express* **9**, 616

- (2001).
- [2] A. G. Markelz, A. Roitberg, and E. J. Heilweil, *Chem. Phys. Lett.* **320**, 42 (2000).
- [3] M. Walther, B. Fischer, M. Schall, H. Helm, and P. U. Jepsen, *Chem. Phys. Lett.* **332**, 389 (2000).
- [4] M. Brucherseifer, M. Nagel, P. H. Bolivar, H. Kurz, A. Bosserhoff, R. Buttner, *Appl. Phys. Lett.* **77**, 4049 (2000).
- [5] R. M. Woodward, B. E. Cole, V. P. Wallace, R. J. Pye, D. D. Arnone, E. H. Linfield, M. Pepper, *Phys. Med. Biol.* **47**, 3853 (2002).
- [6] J. Nishizawa, T. Sasaki, K. Suto, T. Yamada, T. Tanabe, T. Tanno, T. Sawai, Y. Miura, *Opt. Commun.* **244**, 469 (2005).
- [7] R. M. Woodward, V. P. Wallace, R. J. Pye, B. E. Cole, D. D. Arnone, E. H. Linfield, M. Pepper, *J. Invest. Derm.* **120**, 72 (2003).
- [8] B. E. Cole, R. M. Woodward, D. Crawley, *Proc. SPIE* **4276**, 1 (2001).
- [9] E. R. Brown, J. E. Bjarnason, A. M. Fedor, T. M. Korter, *Appl. Phys. Lett.* **90**, 061908 (2007).
- [10] Z. Yan, D. Hou, P. Huang, B. Cao, G. Zhang, Z. Zhou, *Meas. Sci. Technol.* **19**, 015602 (2008).
- [11] J. Xu, K. W. Plaxco, S. J. Allen, *Protein Sci.*, **15**, 1175 (2006).
- [12] B. Fischer, M. Hoffmann, H. Helm, *Optics Express* **13**, 5205 (2005).
- [13] W. Withayachumnankul, B. M. Fischer, D. Abbott, *Proceedings of the Royal Society A: Mathematical, Physical & Engineering Sciences* **464**, 2435 (2008).

*Corresponding author: traian.dascalu@inflpr.ro